Optimal control theory for a target state distributed in time: Optimizing the probe-pulse signal of a pump-probe-scheme

Andreas Kaiser[a] and Volkhard May
Humboldt-Universität zu Berlin, Institut für Physik, Newtonstraße 15, D-12489 Berlin, Germany

(Received 5 April 2004; accepted 17 May 2004)

Optimal control theory (OCT) is formulated for the case of a two-color pump-probe experiment. The approach allows to calculate the pump-pulse shape in such a way that the probe-pulse absorption signal is maximized. Since the latter quantity is given by the time-averaged expectation value of a time dependent operator (the probe-pulse field-strength times the dipole operator) a version of OCT has to be used where the target state is distributed in time. The method is applied to a molecular three-level system with the pump-pulse driving the transition from the electronic ground state into the first-excited electronic state and the probe-pulse connecting the first-excited state with a higher lying electronic state. Depending on the probe-pulse duration, the vibrational wave packet becomes localized or at least highly concentrated in the Franck-Condon window for the transition into the higher-excited state. The dependence on the probe-pulse duration and on the delay time between the optimized pump-pulse and the probe-pulse is discussed in detail. The whole study demonstrates the feasibility of laser pulse induced temporal wave packet localization and the use of spectroscopic quantities as target states in experiments on femtosecond laser pulse control.
 [DOI: 10.1063/1.1769370]

I. INTRODUCTION

Among the various attempts undertaken to achieve femtosecond laser pulse control of molecular dynamics those experiments are of particular interest which also take an optical signal as the observable to be maximized in a feedback-controlled self-learning loop.[1–3] As in other cases these learning loops follow the general suggestion of Ref. 4 and consist of a pulse shaper, a device to measure the signal to be optimized, and an evolutionary algorithm. The latter notices the measured signal and realizes a feedback by iteratively optimizing the exciting laser pulse.

A transient absorption signal from the S_1 level into a higher-excited singlet level of a carotenoid has been used in Ref. 1 to control energy flow pathways in the light-harvesting antenna complex LH2. Selected vibrational mode excitation of crystalline polydiacetylene was demonstrated in Ref. 2 with the feedback signal derived from that of a coherent anti-Stokes Raman scattering setup. Luminescence radiation has been taken in Ref. 3 to maximize the population of a long-lived charge-transfer state in a charge-transfer coordination complex. All these approaches demonstrated the feasibility of optical detection within optical control and represent an alternative to the maximization of, for example, an observable derived from mass spectroscopy (cf., e.g., Ref. 5).

It is the aim of this paper to demonstrate that spectroscopic signals can also be incorporated into the theoretical tool used to study femtosecond laser pulse experiments, i.e., into the optimal control theory (OCT).[6–9] To begin with we will concentrate on a sufficient simple reference example and study a pump-probe scheme in a molecular system with the pump beam driving population into the first-excited state and the probe beam testing the resulting vibrational wave packet motion in this first-excited state via a transition into a higher-excited state (cf. Fig. 1). The control task to be addressed will be the search for the optimal pump-pulse which maximizes the probe-pulse signal.[10] In particular it will be of interest in which manner the probe-pulse duration influences the wave packet formation by the pump pulse. As it is already obvious at this point such a control task has to be based on OCT for the case of a target state distributed in time (see Refs. 11–17 and Appendix A, by the way, this is just the point which essentially improves the investigations of Ref. 10).

In order to determine the probe-pulse signal in a pump-probe scheme one usually calculates[18]

$$S_{\mathrm{pr}} = -\int d\tau \frac{\partial \mathbf{E}_{\mathrm{pr}}(\tau)}{\partial \tau} \mathbf{P}_{\mathrm{pr}}(\tau), \tag{1}$$

with $\mathbf{E}_{\mathrm{pr}}$ and $\mathbf{P}_{\mathrm{pr}}$ denoting the field strength of the probe pulse and the probe-pulse induced polarization, respectively. The latter quantity has to be properly deduced from the expectation value of the dipole operator $\hat{\boldsymbol{\mu}}$ given at the absence of dissipation and for zero temperature as $\langle \Psi(\tau)|\hat{\boldsymbol{\mu}}|\Psi(\tau)\rangle$ where the state vector $|\Psi(\tau)\rangle$ follows from the solution of the time-depending Schrödinger equation including the applied fields (we will comment on this in more detail below).

If one takes S_{pr} as the quantity to be maximized in a control scheme it becomes immediately obvious that the first part of the standard control functional has to be generalized to

$$J_0(\mathbf{E}) = \int d\tau \langle \Psi(\tau;\mathbf{E})|f(\tau)\hat{O}|\Psi(\tau;\mathbf{E})\rangle. \tag{2}$$

[a]Electronic mail: andreas.kaiser@physik.hu-berlin.de

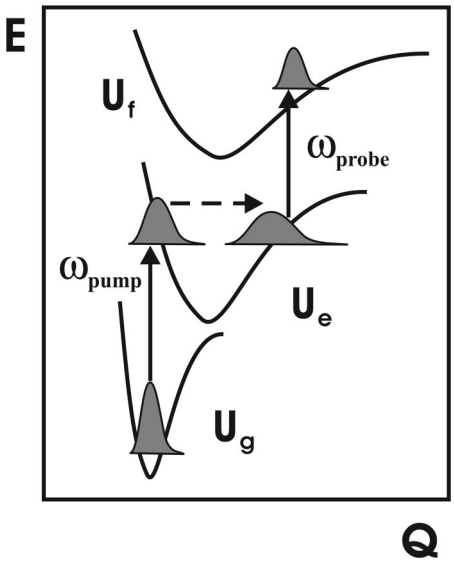

FIG. 1. PES referring to the discussed three-level model.

The quantity $\hat{O}$ is known as the target operator.[6–9] Its time distribution is described by the ordinary time-dependent function $f(\tau)$. Moreover, the dependence on the control field $\mathbf{E}$ is explicitly indicated. Of course, the constraint which guarantees a finite field strength of $\mathbf{E}$ has to be added. The concrete relation between J_0 as well as $f(\tau)\hat{O}$ and the probe-pulse signal S_{pr}, Eq. (1), will be given below.

Once we set $f(\tau)=\delta(\tau-t_f)$ the standard form of $J_0(\mathbf{E})$ is recovered which tries to let become the expectation value of $\hat{O}$ at time t_f as large as possible. In this case the control field which solves the respective control task (the optimal pulse) has to be determined from

$$\mathbf{E}(t)=-\frac{2}{\hbar\lambda}\,\mathrm{Im}\langle\Theta(t;\mathbf{E})|\hat{\boldsymbol{\mu}}|\Psi(t;\mathbf{E})\rangle. \tag{3}$$

The penalty factor λ follows from the constraint of finite field strength and the quantity

$$|\Theta(t;\mathbf{E})\rangle=U(t,t_f;\mathbf{E})\hat{O}|\Psi(t_f;\mathbf{E})\rangle \tag{4}$$

can be understood as the state vector which has to be propagated backwards in time. This backward propagation (from t_f to the earlier time t) is carried out by the time-evolution operator $U(t,t_f;\mathbf{E})$ including the control field. Since the backward propagation of $|\Theta(t;\mathbf{E})\rangle$ is connected with the forward propagation of $|\Psi(t;\mathbf{E})\rangle$ by the field strength as given in Eq. (3), an iteration scheme for the optimal pulse can be established.[19,20]

Considering J_0 according to Eq. (2), one can presume that the generalization of $|\Theta(t)\rangle$, which is propagated backwards when the extremum of the time-nonlocal control functional has to be determined, follows from a time integration with respect to t_f weighted by $f(t_f)$. Therefore, we set ($t_f\rightarrow\tau$)

$$|\tilde{\Theta}(t;\mathbf{E})\rangle=\int d\tau\theta(\tau-t)U(t,\tau;\mathbf{E})f(\tau)\hat{O}|\Psi(\tau;\mathbf{E})\rangle, \tag{5}$$

where $\theta(\tau-t)$ denotes the unit-step function. And indeed, the control problem with the control functional J_0 according to Eq. (2) results in a generalization of Eq. (3) determining the optimal pulse with $|\tilde{\Theta}(t)\rangle$ replacing $|\Theta(t)\rangle$. This is shortly demonstrated in Appendix A but can also be found in Refs. 11–17. For a pump-probe experiment, this concept will be utilized in the following to optimize the pump pulse such that the probe-pulse signal S_{pr} is maximized.

II. THE MODEL AND SOME COMPUTATIONAL DETAILS

As already indicated we will deal with a molecular system characterized by three electronic states φ_a with $a=g$ for the ground state, $a=e$ for the first excited state, and $a=f$ for a higher-excited state. The probe pulse drives a transition into the latter state from φ_e whereas the pump pulse to be optimized populates φ_e via a transition from φ_g. Such a choice is justified if we assume that the energy difference between φ_f and φ_e is very different from that between φ_e and φ_g. The respective Hamiltonian reads

$$H(t;\mathbf{E})=\sum_a H_a(Q)|\varphi_a\rangle\langle\varphi_a|-\mathbf{E}(t)\cdot\hat{\boldsymbol{\mu}}, \tag{6}$$

where the total electric field strength $\mathbf{E}(t)=\mathbf{E}_{\mathrm{con}}(t)+\mathbf{E}_{\mathrm{pr}}(t)$ consists of the pump (control) and the probe field strength $\mathbf{E}_{\mathrm{con}}$ and $\mathbf{E}_{\mathrm{pr}}$, respectively. The vibrational Hamiltonian are given by $H_a(Q)$ and we denote the related vibrational eigenfunctions by χ_{aM} (with vibrational quantum number M). For the numerical computations $H_a(Q)$ are specified by choosing harmonic potential energy surfaces (PES) defined versus a single vibrational coordinate: $U_a(Q)=U_a^{(0)}+\hbar\omega_{\mathrm{vib}}(Q-Q^{(a)})^2/2$. $U_a^{(0)}$ and $Q^{(a)}$ define the bottom of the PES and the "horizontal" position, respectively, and ω_{vib} denotes the vibrational frequency equal for all electronic states.

This represents a rather simple model, however, it is valid for a number of two-atomic molecules or cluster, in particular, if the harmonic approximation here used is softened. Since this paper places emphasis on the general aspects of a control task maximizing the transient absorption signal, the use of such a model is well justified. In particular one can carry out a simple eigenstate expansion to determine the time dependence of the laser-pulse driven total wave function. Then, the expansion coefficients $C_{aM}(t)$ can be taken to compute the electronic level populations $P_a(t)$ according to $\Sigma_M|C_{aM}|^2$, or get the probability distribution $P_a(Q,t)$ of the vibrational coordinate. This quantity is obtained from $|\Sigma_M C_{aM}(t)\chi_{aM}(Q)|^2$, and refers to a particular electronic state, thus visualizing respective wave packet motion.

Next we shortly comment on the determination of the probe-pulse signal, Eq. (1), at the presence of the intensive pump (control) field. We have in mind a probe pulse of type

$$\mathbf{E}_{\mathrm{pr}}(t)=\mathbf{e}_{\mathrm{pr}}E_{\mathrm{pr}}(t)e^{-i\omega_{\mathrm{pr}}t}+\mathrm{c.c.}, \tag{7}$$

oscillating with frequency ω_{pr} and having a polarization unit vector $\mathbf{e}_{\mathrm{pr}}$. A cosine-square function is taken as the envelope of the probe pulse with duration τ_{pr} and centered at t_{pr},

$$E_{\mathrm{pr}}(t)=\tfrac{1}{2}E_{\mathrm{pr}}^{(0)}\cos^2(\pi[t-t_{\mathrm{pr}}]/\tau_{\mathrm{pr}}). \tag{8}$$

It is nonzero for $-\tau_{pr}/2 \leqslant t - t_{pr} \leqslant \tau_{pr}/2$ and vanishes otherwise.

There are different ways to determine that part $\mathbf{P}_{pr}$ of the total polarization $\mathbf{P}$ oscillating with the probe-pulse frequency ω_{pr}. One may, first, expand $\mathbf{P}$ with respect to $\mathbf{E}_{pr}$ and, afterwards, deduce $\mathbf{P}_{pr}$.[18] Alternatively, $\mathbf{P}_{pr}$ may be derived from Schrödinger equations propagated with different phase factors at the molecule-field coupling.[21] A similar approach based on a systematic expansion of $\mathbf{P}_{pr}$ with respect to the carrier waves might be also possible.[22,23] Here, we follow the last mentioned techniques which have the big advantage to allow a propagation of the time-dependent Schrödinger equation with the full field. In this way the need to compute three-time correlation functions depending on three different time arguments is circumvented. Since the control pulse and the probe pulse are spectrally well separated we set here

$$\mathbf{P}_{pr}(\tau) = n_{mol}[\langle \Psi(\tau;\mathbf{E}_{con}+\mathbf{E}_{pr})|\hat{\boldsymbol{\mu}}|\Psi(\tau;\mathbf{E}_{con}+\mathbf{E}_{pr})\rangle - \langle \Psi(\tau;\mathbf{E}_{con})|\hat{\boldsymbol{\mu}}|\Psi(\tau;\mathbf{E}_{con})\rangle]. \quad (9)$$

This formula gives the probe-pulse polarization via the total polarization in the presence of the control and the probe field is diminished by the polarization induced by the control field alone (second term). Inhomogeneous broadening and random spatial orientation have been neglected. This results in a multiplication of the dipole-operator expectation values with the volume density n_{mol} of the considered molecules.

To define the control functional J_0, Eq. (2), via the probe-pulse absorption, Eq. (1), the function $f(\tau)$ and the operator $\hat{O}$ are directly derived from Eq. (9). We obtain

$$f(\tau) = -2n_{mol}\frac{\partial}{\partial\tau}\mathrm{Re}[E_{pr}(\tau)e^{-i\omega_{pr}\tau}], \quad (10)$$

and

$$\hat{O} = \mathbf{e}_{pr}\cdot\hat{\boldsymbol{\mu}}. \quad (11)$$

Since $\mathbf{P}_{pr}$, Eq. (9), is defined via a difference including wave functions which are propagated with and without the probe field the optimal pump field is determined by

$$\mathbf{E}_{con}(t) = -\frac{2}{\hbar\lambda}\mathrm{Im}[\langle\tilde{\Theta}(t;\mathbf{E}_{con}+\mathbf{E}_{pr})|\hat{\boldsymbol{\mu}}|\Psi(t;\mathbf{E}_{con}+\mathbf{E}_{pr})\rangle - \langle\tilde{\Theta}(t;\mathbf{E}_{con})|\hat{\boldsymbol{\mu}}|\Psi(t;\mathbf{E}_{con})\rangle]. \quad (12)$$

This equation somewhat generalizes Eq. (3) [or Eq. (A4)]. The state vector $|\tilde{\Theta}\rangle$ has to be propagated backwards in time according to the effective and inhomogeneous Schrödinger equation (A5). The time evolution starts at t_∞ (a time much larger than the final time of the probe-pulse action) and with the "initial" value $|\tilde{\Theta}(t_\infty)\rangle = 0$. Since the inhomogeneity $f(t)\hat{O}|\Psi(t)\rangle$ is present (with the concrete form for $f(t)$ and $\hat{O}$ as given above) $|\tilde{\Theta}\rangle$ gets finite values if the time interval is reached where the probe pulse acts. The forward propagation of $|\Psi(t)\rangle$ is determined by the ordinary time-dependent Schrödinger equation with the initial value $|\Psi(t_0)\rangle = |\chi_{g0}\rangle|\varphi_g\rangle$. According to the considered zero-temperature case the system is in the vibrational ground state χ_{g0} of the electronic ground state initially (at a time t_0 before the pump as well as the probe field start to act).

TABLE I. Model parameters referring to the pump-probe scheme of Fig. 1.

a	$U_a^{(0)}$ (eV)	$Q^{(a)}$	$\hbar\omega_{vib}$ (eV)	d_{ab}
g	0	0	0.1	-
e	2	2	0.1	$d_{eg}=2.4$ D
f	3	6	0.1	$d_{fe}=1.6$ D

III. NUMERICAL RESULTS

Before presenting details of our numerical calculations, we further specify the considered model by fixing some parameters (see Table I). They have been taken to comply with a two-color pump-probe experiment, i.e., the energetic distance of the first-excited electronic state to the ground state is different from the distance between the first- and the higher-excited state. Moreover, the equilibrium positions of the respective PESs have been arranged as shown in Fig. 1. In order to probe the system via the transitions from φ_e to φ_f, we take a probe pulse with carrier frequency $\hbar\omega_{pr}=1$ eV and field amplitude $E_{pr}^{(0)}=5\times10^4$ V/cm. The latter value ensures that probe pulse perturbes the system only weakly.

The duration of the optimal pulse will be restricted to the time interval between $t_0=0$ and the final time $t_f=300$ fs. A smooth switch-on and switch-off of the optimal pulse can be achieved by extending the penalty factor λ [cf. Eq. (12)] by a sine-square function $s(t)=\sin^2(\pi t/[t_f-t_0])$, $\lambda\rightarrow\lambda/s(t)$. Moreover, we set λ equal to 5×10^{-6} nm/eV.

First we will consider the case where the duration of the optimal pulse extends up to $t_f=300$ fs and the probe pulse (with a duration of $\tau_{pr}=20$ fs) is centered at $t_{pr}=225$ fs. Since the vibrational oscillation period $T_{vib}=2\pi/\omega_{vib}$ amounts 41 fs (cf. Table I) such a pump-probe configuration allows the molecule to perform several oscillations before the probe pulse acts.

For the described situation Fig. 2 shows the optimal pump pulse and the probe pulse together with the populations of the electronic ground state and of the first-excited state (note that the probe pulse does not induce any noticeable changes of P_e, moreover, $P_f\approx0$, which is not plotted). The optimal pump pulse consists of several subpulses, whose durations reflect the internal vibrational dynamics, and within the first 160 fs it induces a nearly complete population inversion. Correspondingly, the temporal evolution of the population are superposed by oscillations. About 40 fs and 20 fs before the probe pulse starts to act the pump pulse shows two major subpulses, the first strongly depopulates the excited state while the second repopulates it completely. This behavior indicates strong wave function interference induced to maximize the probe-pulse signal. If the probe pulse is over the OCT scheme leads to a switch-off of the pump pulse although it may extend up to $t_f=300$ fs.

Before considering the case of a shorter delay time between probe-pulse action and pump-pulse turn-on we will take a closer look at the wave packet dynamics by analyzing the temporal behavior of $P_e(Q,t)$. This is shown in Fig. 3

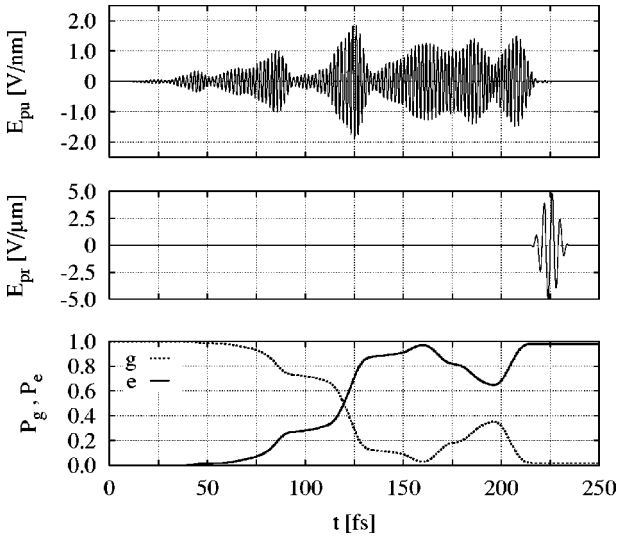

FIG. 2. Field strength of the optimal pump pulse (upper panel) which maximizes the absorption signal of a probe pulse centered at $t_{pr}=225$ fs and with duration $\tau_{pr}=20$ fs (middle panel). The respective ground-state population $P_g(t)$ and the population of the first-excited state $P_e(t)$ are shown, too (lower panel).

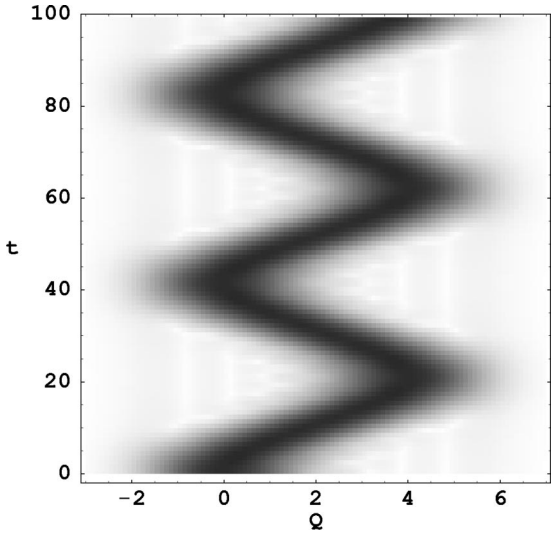

FIG. 4. Probability density $P_e(Q,t)$ of the vibrational wave packet in the first-excited state vs time (in femtoseconds) after impulsive excitation (at $t=0$ and with the wave packet positioned at $Q=0$, the values of P_e are nonlinearly gray scaled, white for zero and black for one).

according to the situation already discussed in Fig. 2. Up to the probe-pulse action around 225 fs one notices certain interference patterns. If the probe pulse maximum is reached $P_e(Q,t)$ becomes almost localized at about $Q=4$ for ≈ 10 fs. This localization guarantees a maximal probe-pulse signal. Afterwards the vibrational wave packet delocalizes. Within the free motion of the system, when the pump and probe-pulse actions are over, the wave packet, interestingly, reassembles its prior prepared localized shape after half the vibrational oscillation period, $T_{vib}/2$ but now mirror inverted at the left border of the PES ($Q\approx 0$). This oscillatory motion with alternating localizations and delocalizations continues with frequency ω_{vib}, indicating that it is originated by the harmonic shape of the PES. This type of (nondriven) propagation differs strongly from that following an impulsive excitation, where the vibrational ground-state wave function $\chi_{g0}(Q)$ is instantaneously positioned at the excited-state PES (cf. Fig. 4). Instead of strong probability concentration around $Q=0$ and 4 as given in Fig. 3 we notice the well-known harmonic wave packet motion with probability concentrated at the center of the wave packet.

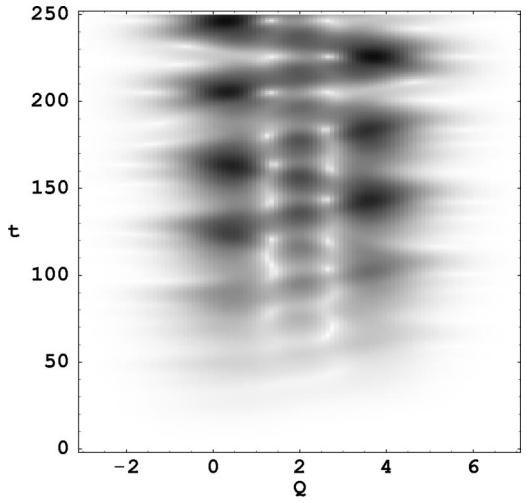

FIG. 3. Probability density $P_e(Q,t)$ of the vibrational wave packet in the first-excited state vs time (in femtoseconds) corresponding to the solution of the control task as given in Fig. 2 (the values of P_e are nonlinearly gray scaled, white for zero and black for one).

When varying the probe-pulse duration τ_{pr}, the optimal pump pulse and the electronic-state populations show the same features as described above, however, the localization of the vibrational wave packet is strongly influenced. For a short probe pulse of $\tau_{pr}=10$ fs the wave packet remains concentrated at $Q=4$ during the whole probe-pulse action. This is illustrated in the upper panel of Fig. 5. When increasing τ_{pr}, this localization survives up to 30 fs.

Relating the structure of the optimal pulse and the temporal behavior of the electronic state populations as shown in Fig. 2 to the characteristic time of molecular dynamics, i.e., to T_{vib}, it should be possible to solve the control task also for a shorter delay (between pump-pulse turn-on and probe-pulse action). The behavior of the system for a smaller time delay with $t_{pr}=75$ is shown in Figs. 6 and 7. Now, the majority of population is transfered to the first-excited state by one large subpulse beginning at $t\approx 40$ fs. This leads to an occupation probability of the state ϕ_e of about 74% which is definitively less than in the case of $t_{pr}=225$ fs. The subpulse also takes care of the localization of the vibrational wave packet at $Q\approx 4$ around $t\approx t_{pr}$. However, a detailed comparison with Fig. 5, middle panel shows that the wave packet concentration remains less sharp when t_{pr} is decreased from 225 fs to 75 fs. This is in general by observed when using OCT theory (cf., e.g., Ref. 24). As long as there is no destructive influence of dissipation the wave packet interference necessary to solve the control task becomes more efficient if the conceded time interval becomes larger.

The mentioned behavior is also found when studying the probe-pulse absorption signal S_{pr}, Eq. (1), in dependence on the time delay between pump-pulse switch-on and the probe-

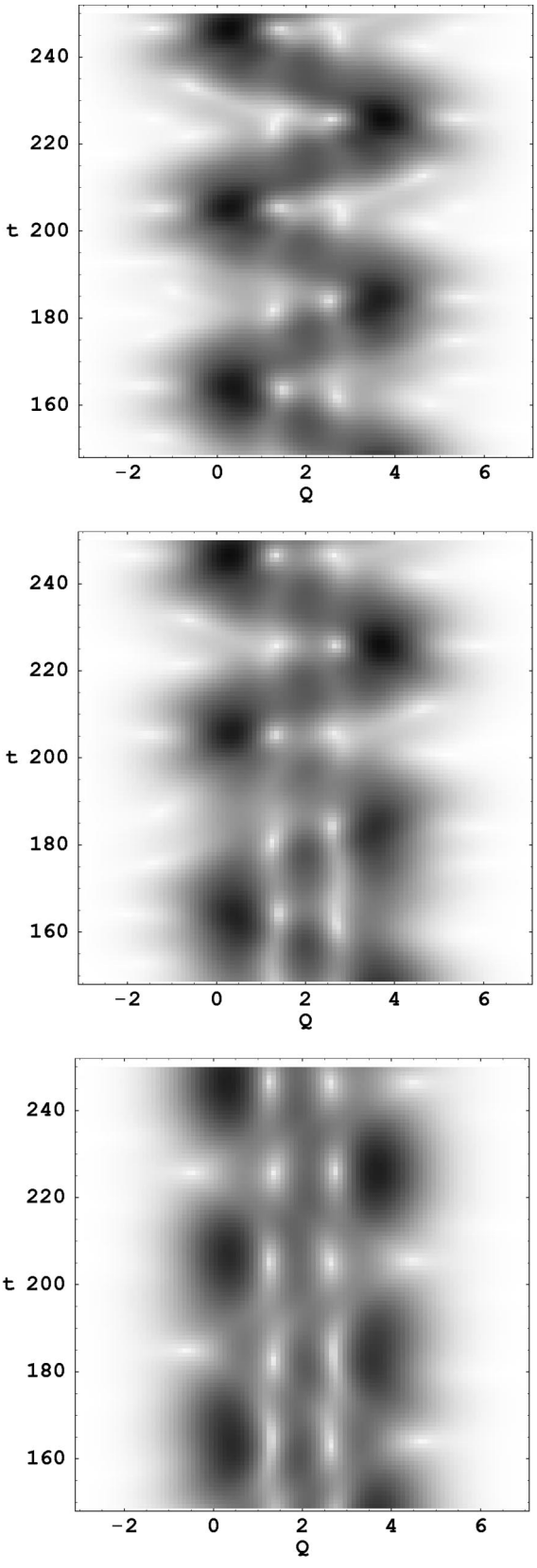

FIG. 5. Probability density $P_e(Q,t)$ of the vibrational wave packet in the first-excited state vs time (in femtoseconds) corresponding to the solution of the control task as given in Fig. 2 but with different values for the probe-pulse durations. Upper panel $\tau_{pr}=10$ fs, middle panel $\tau_{pr}=20$ fs, and lower panel $\tau_{pr}=40$ fs (the values of P_e are nonlinearly gray scaled, white for zero and black for one).

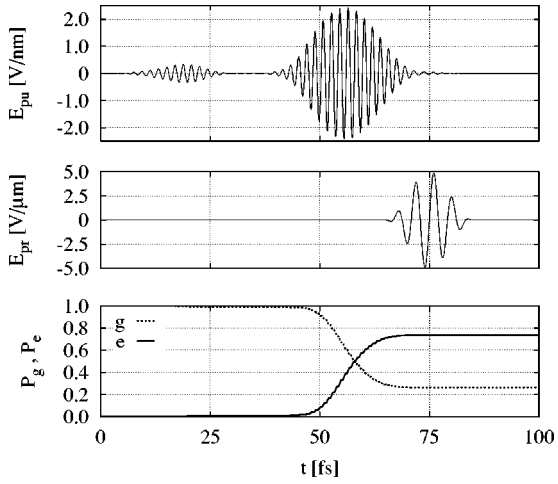

FIG. 6. Field strength of the optimal pump pulse (upper panel) which maximizes the absorption signal of a probe pulse centered at $t_{pr}=75$ fs and with duration $\tau_{pr}=20$ fs (middle panel). The respective ground-state population $P_g(t)$ and the population of the first-excited state $P_e(t)$ are shown, too (lower panel).

pulse action given by t_{pr} as well as in dependence on the probe-pulse width τ_{pr}. For comparison S_{pr} needs to be normalized. With respect to standard OCT a normalization to $\int|f(\tau)|d\tau$ is appropriate. On the other hand, normalizing to the probe-pulse energy flux gives the efficiency of the optimization task, namely, the ratio of the absorped and incomming probe-pulse energy. The latter method will be applied here. For convenience, we approximate the probe-pulse energy flux by $\propto\int E_{pr}^2(\tau)d\tau$. The results are shown in Fig. 8. For a fixed delay time (determined by t_{pr}) S_{pr} increases with the probe-pulse width τ_{pr} and reaches a maximum at about 20 fs. For larger durations the absorption signal decreases. In this regime, the internal molecular dynamics works counteractive by preventing the localization of the vibrational wave

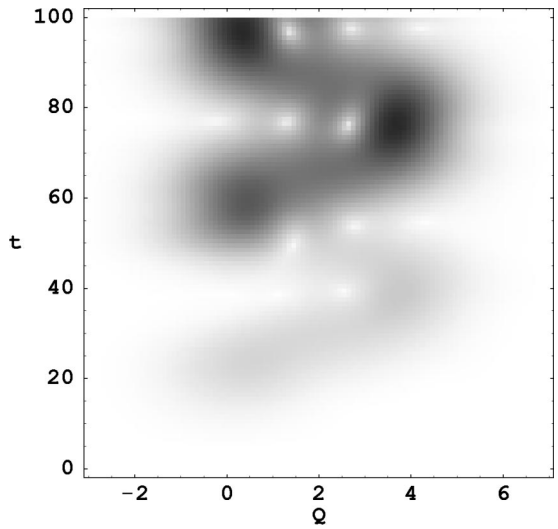

FIG. 7. Probability density $P_e(Q,t)$ of the vibrational wave packet in the first-excited state vs time (in femtoseconds) corresponding to the solution of the control task as given in Fig. 6 (the values of P_e are nonlinearly gray scaled, white for zero and black for one).

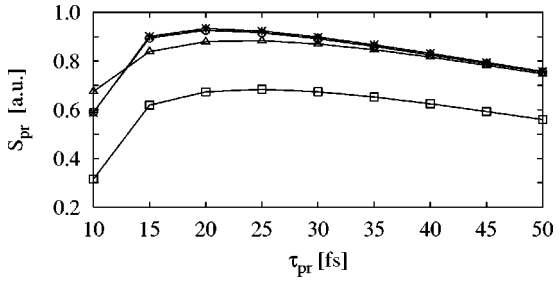

FIG. 8. Probe-pulse absorption signal S_{pr}, Eq. (1) (normalized as explained in the text) as a function of the probe-pulse duration τ_{pr} and for different delay times (see text). Squares: $t_{\mathrm{pr}}=75$ fs, triangles: $t_{\mathrm{pr}}=150$ fs, diamonds: $t_{\mathrm{pr}}=225$ fs, and stars: $t_{\mathrm{pr}}=275$ fs.

packet in the Franck-Condon window during probe pulse which becomes more pronounced with larger τ_{pr}. Furthermore, for probe-pulse length larger than 10 fs. Figure 8 indicates an increase of S_{pr} with the delay time (t_{pr}) which finally saturates if t_{pr} exeeds 200 fs.

Within the parameter regime considered above, the probe pulse only connects the states φ_e and φ_f while the pump pulse drives transitions between φ_g to φ_e. This has been checked by calculations where the probe and the pump pulse couple only to the corresponding transition dipole elements d_{ef} and d_{ge}, respectively.

When the probe-pulse duration becomes 10 fs or less, one enters a regime where the frequency broadening is large enough to also allow for transitions between φ_g and φ_e. In Fig. 9 the optimal pump pulse and the populations of the electronic states are shown for the same parameters as in Fig. 2 but with a probe-pulse duration of $\tau_{\mathrm{pr}}=5$ fs. Interestingly, the optimal pump pulse also slightly populates the higher-excited state φ_f (note the increased carrier frequency around 200 fs). In contrast to the case of $\tau_{\mathrm{pr}}=20$ fs the ground state is first depopulated and then repopulated when the probe pulse acts. This behavior is typical when the target state is positioned in the ground state. Surprisingly, a localization of

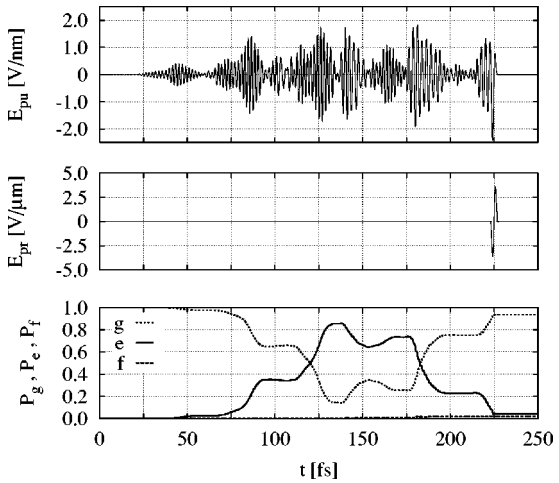

FIG. 9. Field-strength of the optimal pump-pulse (upper panel) which maximizes the absorption signal of a probe pulse centered at $t_{\mathrm{pr}}=225$ fs and with duration $\tau_{\mathrm{pr}}=5$ fs (middle panel). The respective ground-state population $P_g(t)$, the population of the first-excited state $P_e(t)$ and second-excited state $P_f(t)$ are shown, too (lower panel).

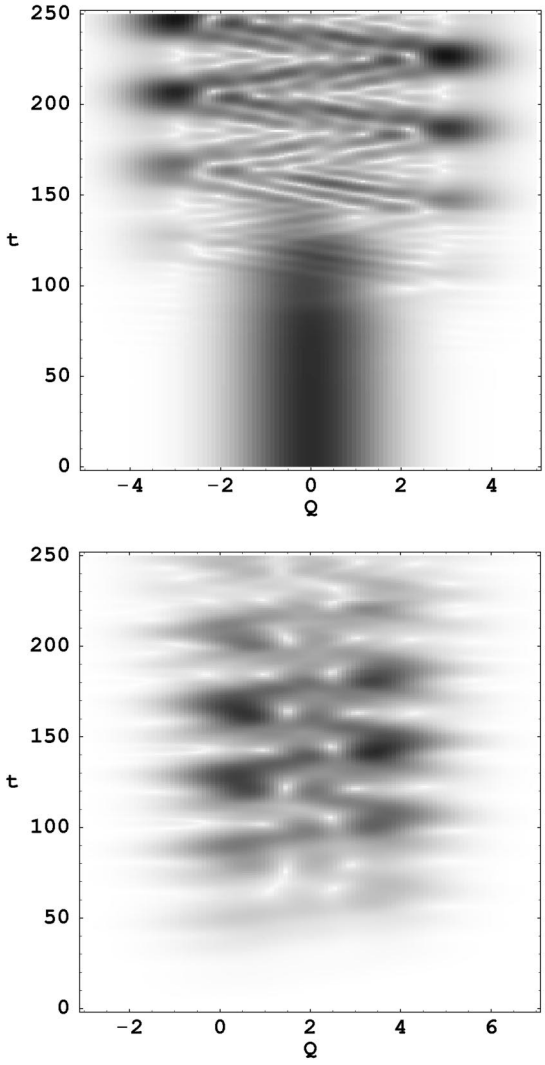

FIG. 10. Probability density $P_g(Q,t)$ of the vibrational wave packet in the ground state (upper panel) and $P_e(Q,t)$ of the vibrational wave packet in the first-excited state (lower panel) vs time (in femtoseconds) corresponding to the solution of the control task as given in Fig. 9. (The values of P_e are nonlinearly gray scaled, white for zero and black for one.)

the vibrational wave packet in the first-excited state, contributing additionally to the absorption signal, does not take place (See Fig. 10). Considering nonoverlapping pulses, such a behavior has also been observed when $U_f^{(0)}$ is shifted to 3.5 eV and an appropriate carrier frequence for the probe pulse is chosen. Only if τ_{pr} becomes larger, the wave packet of state e begins to concentrate in the Franck-Condon window as well. However, the population of the first-excited state is still neglectible compared with the ground-state population.

Finally, a modified system defined by the parameters given in Table I but with the second-excited PES horizontally shifted between the ground-state PES and the first-excited state PES ($Q^{(f)}=1$) is investigated. Similar as above, the optimal pump pulse creates a localized wave packet in the first-excited state within the Franck-Condon window of the probe pulse, which lies at about the center of the PES of the first-excited state, illustrated in Fig. 11. Here, the excited wave packet is stonger localized by the optimal pulse than in

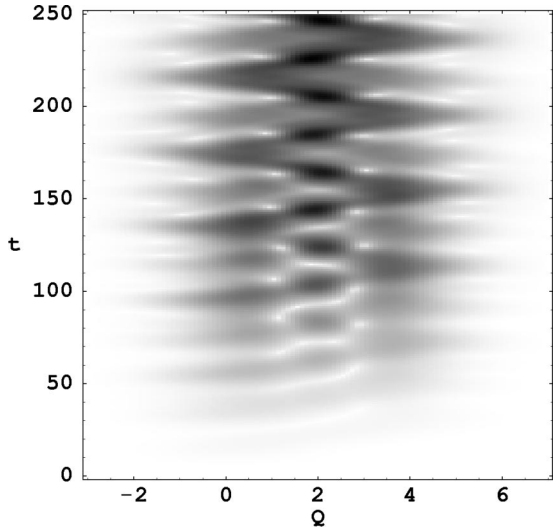

FIG. 11. Probability density $P_e(Q,t)$ of the vibrational wave packet in the first-excited state vs time (in femtoseconds) corresponding to the solution of the control task for $t_{pr}=225$ fs and $\tau_{pr}=20$ fs using the system parameters given in Table I but with $Q^{(f)}=1$. (The values of P_e are nonlinearly gray scaled, white for zero and black for one.)

the above discussed case. When increasing the probe-pulse duration, the shape of the wave packet broadens, however, the side oscillations in the wave functions are mostly suppressed. This leads to larger absorption signals than for the prior considered system. Furthermore, for this modified model system the probe-pulse absorption signal increases with the probe-pulse length, shown in Fig. 12. This indicates that the counteracting impact of the molecular dynamics on the localization of a wave packet at the center of the PES is significantly smaller than at the boundries.

IV. CONCLUSIONS

Considering a standard pump-probe experiment we have presented a formulation of OCT which enables the calculation of an *optimal* pump pulse which prepares the molecular system such that the probe-pulse absorption signal is maximized. This spectroscopic signal is given by the time-integrated expectation value of a time-dependent operator proportional to the (time derivative of the) probe field-strength time of the dipole operator. Accordingly the optimal pump pulse (control pulse) has to move the system into a certain state not only at a specific time but within a certain time interval. Such a target state distributed in time can be accounted for by a particular inhomogeneity in the effective Schrödinger equation which executes the OCT propagation backward in time.

The resulting effect is remarkable and has been demonstrated for a molecular system with three electronic states defined versus a single vibrational coordinate. For probe pulses shorter than the oscillation period of the vibrational coordinate, the optimal pump pulse induces spatial and temporal wave packet localization in the excited electronic state just to have it in the Franck-Condon window for probe-pulse absorption at the presence of this pulse. When the probe-pulse duration becomes comparable or larger than the oscillation period of the vibrational coordinate, the intramolecular dynamics hampers the further localization of the wave packet. Correspondingly the probe-pulse absorption signal first increases with the probe-pulse duration and at a certain pulse duration, which in our model lies around the half of the vibrational oscillation period, decreases again. Furthermore, the shaping of the wave packet for optimal absorption requires a certain amount of time. Thus, the probe-pulse absorption signal increases with an increase of the time delay between the pump-pulse switch on and the probe pulse but finally it saturates.

The presented results here give a first impression of the processes taking place when laser pulse control is performed with respect to spectroscopic signals. In this connection a molecular system might be set into a specific target state with an almost localized wave packet positioned. However, for comparison with experiments a more realistic model has to be considered, in particular, anharmonic PESs have to be used which, e.g., will alter the propagation of the vibrational wave packet in the excited PES. Furthermore, the optimization of a probe signal in a selected frequency interval using broadband transient absorption signals (see Appendix) is of high interest as well. Both questions are objects of currently on-going work.

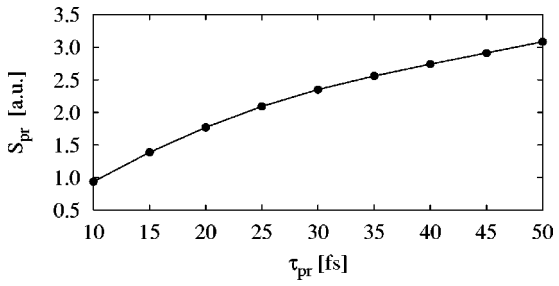

FIG. 12. Probe-pulse absorption signal S_{pr}, Eq. (1) (normalized as explained in the text) as a function of the probe-pulse duration τ_{pr} corresponding to the solution of the control task for $t_{pr}=225$ fs using the system parameters given in Table I but with $Q^{(f)}=1$.

ACKNOWLEDGMENT

We gratefully acknowledge support by the Deutsche Forschungsgemeinschaft through Sfb 450.

APPENDIX A: OPTIMAL CONTROL THEORY FOR A TARGET STATE DISTRIBUTED IN TIME

In the following we demonstrate that indeed the backward propagation of $|\tilde{\Theta}\rangle$, Eq. (5), solves the control problem which has been set up by the control functional J_0, Eq. (2). Similar control functionals (including a time integral with respect to the systems wave function) can also be found in Refs. 11–17 with the aim of suppressing an ''undesirable'' operator $\hat{O}$[11,12] or to constrain the time evolution of intermediate states.[13] However, only the simplified versions of Refs. 15–17 entered explicit numerical calculations.

Since our total control functional

$$J(\mathbf{E}) = J_0(\mathbf{E}) - \frac{\lambda}{2}\int d\tau \mathbf{E}^2(\tau) \tag{A1}$$

differs somewhat from those used in Refs. 11–17 (the time-dependent Schrödinger equation does not appear explicity as a constraint, for example) we briefly repeat the determination of the optimal pulse. The search for the extremum of J gives an equation for the optimal field determined via $\delta J/\delta \mathbf{E}(t) = 0$. To compute the functional derivative (or Fréchet derivative) we note

$$\frac{\delta}{\delta \mathbf{E}(t)} U(\tau, t_0; \mathbf{E}) = \frac{i}{\hbar}\theta(\tau - t) U(\tau, t; \mathbf{E}) \hat{\boldsymbol{\mu}} U(t, t_0; \mathbf{E}), \tag{A2}$$

where $U(\tau, t_0; \mathbf{E})$ is the total time-evolution operator. The (functional) equation for the optimal pulse takes the form

$$\mathbf{E}(t) = -\frac{2}{\hbar\lambda}\mathrm{Im}\int d\tau \theta(\tau - t) \times \langle \Psi(\tau; \mathbf{E}) | f(\tau) \hat{O} U(\tau, t; \mathbf{E}) \hat{\boldsymbol{\mu}} | \Psi(t; \mathbf{E}) \rangle, \tag{A3}$$

which is identical with

$$\mathbf{E}(t) = -\frac{2}{\hbar\lambda}\mathrm{Im}\langle \tilde{\Theta}(t; \mathbf{E}) | \hat{\boldsymbol{\mu}} | \Psi(t; \mathbf{E}) \rangle, \tag{A4}$$

if $|\tilde{\Theta}(t; \mathbf{E})\rangle$ has been defined according to Eq. (5). This immediately gives the following equation:

$$\frac{\partial}{\partial t}|\tilde{\Theta}(t)\rangle = -\frac{i}{\hbar} H(t) |\tilde{\Theta}(t)\rangle - f(t)\hat{O}|\Psi(t)\rangle. \tag{A5}$$

In contrast to Eq. (4) for $|\Theta(t; \mathbf{E})\rangle$, it is an inhomogeneous time-dependent Schrödinger equation with an inhomogeneity which represents the target operator distributed in time.

APPENDIX B: OPTIMIZING PROBE-PULSE ABSORPTION IN THE FREQUENCY DOMAIN

Instead of using Eq. (1) where the probe-pulse signal S_{pr} is represented by a time integral with respect to $S_{\mathrm{pr}}(\tau) = -\mathbf{P}_{\mathrm{pr}} \partial \mathbf{E}_{\mathrm{pr}}/\partial\tau$ one can also change to the frequency domain. Now we write

$$S_{\mathrm{pr}} = \int d\omega S_{\mathrm{pr}}(\omega) \tag{B1}$$

with $S_{\mathrm{pr}}(\omega) = i\mathbf{P}_{\mathrm{pr}}(-\omega)\omega \mathbf{E}_{\mathrm{pr}}(\omega)/2\pi$ defined by the Fourier-transformed fields. In this case one may ask if it would be possible to maximize $S_{\mathrm{pr}}(\omega)$ not along the whole frequency axis but within a certain frequency interval $\Delta\omega$ around ω_0. One immediately notices that in such a case one has to replace the function $f(\tau)$ given in Eq. (10) by

$$f(\tau) = -n_{\mathrm{mol}} \int_{\omega_0 - \Delta\omega/2}^{\omega_0 + \Delta\omega/2} \frac{d\omega}{2\pi i} e^{-i\omega\tau} \mathbf{e}_{\mathrm{pr}} \mathbf{E}_{\mathrm{pr}}(\omega). \tag{B2}$$

The probe field is represented by its *incomplete* inverse Fourier transform, obtained from an integration with respect to the frequency interval in which $S_{\mathrm{pr}}(\omega)$ should become maximal.

[1] J. L. Herek, W. Wohlleben, R. J. Cogdell, D. Zeidler, and M. Motzkus, Nature (London) **417**, 533 (2002).
[2] D. Zeidler, S. Frey, W. Wohlleben, M. Motzkus, F. Busch, T. Chen, W. Kiefer, and A. Materny, J. Chem. Phys. **116**, 5231 (2002).
[3] T. Brixner, N. H. Damrauer, B. Kiefer, and G. Gerber, J. Chem. Phys. **118**, 3692 (2003).
[4] R. S. Judson and H. Rabitz, Phys. Rev. Lett. **68**, 1500 (1992).
[5] C. Daniel, J. Full, L. González, C. Lupulescu, J. Manz, A. Merli, S. Vajda, and L. Wöste, Science **299**, 536 (2003).
[6] A. P. Pierce, M. A. Dahleh, and H. Rabitz, Phys. Rev. A **37**, 4950 (1988).
[7] S. A. Rice and M. Zhao, *Optical Control of Molecular Dynamics* (Wiley, New York, 2000).
[8] M. Shapiro and P. Brumer, *Principles of the Quantum Control of Molecular Processes* (Wiley, New Jersey, 2003).
[9] V. May and O. Kühn, *Charge and Energy Transfer Dynamics in Molecular Systems* (Wiley-VCH, Berlin, 2004).
[10] Z. Shen, V. Engel, R. Xu, and Y. Yan, J. Chem. Phys. **117**, 6142 (2002).
[11] M. Demiralp and H. Rabitz, Phys. Rev. A **47**, 809 (1993).
[12] M. Demiralp and H. Rabitz, Phys. Rev. A **57**, 2420 (1998).
[13] Y. Ohtsuki, K. Nakagami, Y. Fuijimura, W. Zhu, and H. Rabitz, J. Chem. Phys. **114**, 8867 (2001).
[14] Y. Ohtsuki, G. Turinici, and H. Rabitz, J. Chem. Phys. **120**, 5509 (2004).
[15] S. Shi and H. Rabitz, J. Chem. Phys. **92**, 364 (1990).
[16] S. Shi and H. Rabitz, J. Chem. Phys. **97**, 276 (1992).
[17] H. Zhang and H. Rabitz, J. Chem. Phys. **101**, 8580 (1994).
[18] S. Mukamel, *Principles of Nonlinear Optical Spectroscopy* (Oxford University Press, Oxford, 1999).
[19] W. Zhu, J. Botina, and H. Rabitz, J. Chem. Phys. **108**, 1953 (1998).
[20] W. Zhu and H. Rabitz, J. Chem. Phys. **109**, 385 (1998).
[21] L. Seidner, G. Stock, and W. Domcke, J. Chem. Phys. **103**, 3998 (1995).
[22] Th. Renger and V. May, J. Phys. Chem. A **102**, 4381 (1998).
[23] Th. Renger, V. May, and O. Kühn, Phys. Rep. **343**, 137 (2001).
[24] T. Mancal, U. Kleinekathöfer, and V. May, J. Chem. Phys. **117**, 636 (2002).